# Single-Crystal Structures, Optical Absorptions, and Electronic Distributions of Thorium Oxychalcogenides ThOQ (Q = S, Se, Te)

Lukasz A. Koscielski,[†] Emilie Ringe,[†] Richard P. Van Duyne,[†] Donald E. Ellis,[†,‡] and James A. Ibers*,[†]

[†]Department of Chemistry and [‡]Department of Physics and Astronomy, Northwestern University, 2145 Sheridan Road, Evanston, Illinois 60208, United States

S *Supporting Information*

ABSTRACT: The compounds ThOS, ThOSe, and ThOTe have been synthesized, and their structures have been determined by means of single-crystal X-ray diffraction methods. All three compounds adopt the PbFCl structure type in the tetragonal space group $D_{4h}^7 - P4/nmm$. More precise crystallographic data have been obtained for ThOS and ThOSe, which had previously only been known from X-ray powder diffraction data. ThOS, ThOSe, and ThOTe are yellow-, orange-, and black-colored, respectively. From single-crystal optical absorption measurements the band gaps are 2.22, 1.65, and 1.45 eV, respectively. Optical band gaps, ionic charges, and densities of states were calculated for the three compounds with the use of Density Functional methods.
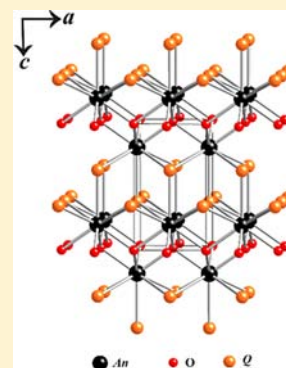
INTRODUCTION

The ThOQ (Q = S, Se, Te) compounds are isostructural to other AnOQ (An = U, Np, Pu) compounds,[1−4] and crystallize in the PbFCl structure type in space group $D_{4h}^7 - P4/nmm$ of the tetragonal system. The structure differs from those of the parent ThQ$_2$ compounds. ThS$_2$ and ThSe$_2$ crystallize in the orthorhombic space group *Pmna*, and ThTe$_2$, from X-ray powder diffraction data, appears to crystallize in the hexagonal system with cell constants $a = 8.49$ Å and $c = 9.01$ Å.[5−7] The ThOQ compounds were first identified and characterized structurally from X-ray powder diffraction data.[8,9] In addition, the structure of ThOTe has been characterized by single-crystal X-ray diffraction methods.[10] Since then, there have been numerous studies of these compounds, including their syntheses, structures (including those at high pressures), doping properties, and thermal properties.[9,11−15] However, no optical measurements have been performed on ThOQ compounds despite their bright colors, nor have theoretical studies been performed.

Here we report single-crystal X-ray diffraction structures of all three compounds as well as their optical properties and computational results on electronic distributions and densities of states.

EXPERIMENTAL METHODS

Caution! ^{232}Th *is an α-emitting radioisotope and as such is considered a health risk. Its use requires appropriate infrastructure and personnel trained in the handling of radioactive materials.*

Syntheses. Fe (Aesar, 99.5%), Ge (Aldrich, 99.99%), S (Mallinckrodt, 99.6%), Se (Cerac, 99.999%), Te (Aldrich, 99.8%), NaBr (Aldrich, 99.99+%), and CsCl (Aldrich, 99.9%) were used as received. Two sources of Th were used: Th (MP Biomedicals) and Th

chunks (Albrecht-Schmitt, Notre Dame) powdered according to a literature procedure.[16] Both sources yielded ThOQ crystals.

The ThOQ compounds were synthesized as side products in multiple reactions. Although other reactants were present, the elemental compositions of the crystals were determined to be only Th/O/Q on an EDX-equipped Hitachi S-3400 SEM. The crystals were generally plate-like and were yellow, orange, or black for Q = S, Se, or Te, respectively.

Listed below is one reaction for each chalcogen. Reactants were loaded into carbon-coated fused-silica tubes in an Ar-filled glovebox. Each tube was evacuated to near 10^{-4} Torr, flame-sealed, placed in a computer-controlled furnace, and then heated according to the specified temperature profile.

ThOS. A tube was loaded with Th (30.0 mg, 0.129 mmol), Ge (9.4 mg, 0.129 mmol), S (4.2 mg, 0.131 mmol), and NaBr (53.2 mg, 0.517 mmol). It was heated to 1273 K in 24 h, kept at 1273 K for 99 h, cooled to 673 in 198 h, and then cooled to 298 K in 4 h. The tube contained a yellow-colored amorphous solid and many well-formed yellow plates of ThOS.

ThOSe. A tube was loaded with Th (30 mg, 0.129 mmol), Fe (7.2 mg, 0.129 mmol), Se (30.6 mg, 0.388 mmol), and CsCl (100 mg, 0.594 mmol). It was heated to 1173 K in 30 h, kept at 1173 K for 96 h, cooled to 773 K in 144 h, kept at 773 K for 48 h, and then cooled to 298 K in 6 h. The tube contained orange crystals of ThOSe and metallic pieces, which by EDX examination contained Cs, Fe, and Se.

ThOTe. A tube was loaded with Th (30.0 mg, 0.129 mmol) and Te (33.0 mg, 0.258 mmol). It was heated to 1273 K in 24 h, kept at 1273 K for 72 h, and then cooled to 298 K in 9 h. The tube contained black plates of ThOTe in nearly 100 wt % yield and some black powder, which was identified as ThOTe by an X-ray powder diffraction measurement.

Crystal Structure Determinations. Single-crystal X-ray diffraction data for ThOQ (Q = S, Se, Te) were collected with the use of graphite-monochromatized MoKα radiation (λ = 0.71073 Å) at 100 K on a Bruker APEX2 diffractometer.[17] For ThOS and ThOSe, data were collected by a scan of 0.3° in ω in groups of 606 frames at φ settings of 0°, 90°, 180°, and 270°. Crystal decay was monitored by recollecting 50 initial frames at the end of the data collection. For ThOTe the data collection strategy was obtained from an algorithm in COSMO in the program APEX2[17] as a series of 0.3° scans in φ and ω. For all data collections the crystal-to-detector distance was 6.0 cm and the exposure time was 10 s/frame. The collection of intensity data as well as cell refinement and data reduction were carried out with the use of the program APEX2.[17] Face-indexed absorption, incident beam, and decay corrections were performed with the use of the program SADABS.[18] The structures were solved with the direct-methods program SHELXS and refined with the least-squares program SHELXL.[19] The atomic positions were standardized with the program STRUCTURE TIDY.[20] Additional experimental details are given in Table 1 and in the Supporting Information.

Table 1. Crystal Data and Structure Refinements for ThOQ[a]

compound	ThOS	ThOSe	ThOTe
color	yellow	orange	black
Fw	280.10	327.00	375.64
a (Å)	3.9580(2)	4.0176(4)	4.1173(3)
c (Å)	6.7468(3)	7.0198(6)	7.5289(6)
V (Å^3)	105.694(9)	113.31(2)	127.63(2)
ρ_c (g cm^{-3})	8.801	9.584	9.775
μ (mm^{-1})	71.08	81.45	69.25
$R(F)^b$	0.0134	0.0177	0.0130
$R_w(F^2)^c$	0.0298	0.0455	0.0345

[a]For all structures Z = 2, space group = P4/nmm, λ = 0.71073 Å, T = 100(2) K. [b]$R(F) = \sum ||F_o| - |F_c||/\sum |F_o|$ for $F_o^2 > 2\sigma(F_o^2)$. [c]$R_w(F^2) = \{\sum [w(F_o^2 - F_c^2)^2]/\sum wF_o^4\}^{1/2}$ for all data. $w^{-1} = \sigma^2(F_o^2) + (qF_o^2)^2$ for $F_o^2 \geq 0$; $w^{-1} = \sigma^2(F_o^2)$ for $F_o^2 < 0$. q = 0.0127 for ThOS, 0.0249 for ThOSe, and 0.0135 for ThOTe.

Optical Measurements. Single-crystal optical absorption measurements were performed at visible frequencies from 3.2 eV (387 nm) to 1.5 eV (827 nm) and at IR frequencies from 1.8 eV (668 nm) to 1.08 eV (1148 nm) at 298 K. A single crystal of ThOQ (Q = S, Se, Te) mounted on a goniometer head was inserted on a custom-made holder fitted to a Nikon Eclipse Ti2000−U inverted microscope. The crystal was positioned at the focal plane above the 20× objective of the microscope and illuminated with a tungsten-halogen lamp. The transmitted light was spatially filtered with a 200 μm aperture. For visible measurements, light was dispersed by a 150 groove/mm grating in an Acton SP2300i imaging spectrometer, and collected on a back-illuminated, liquid nitrogen-cooled CCD (Spec10:400BR, Princeton Instruments). For IR measurements, light was dispersed by a 150 groove/mm grating in an Acton SP2300i imaging spectrometer configured for IR wavelengths, and collected on a liquid nitrogen-cooled InGaAs Array detector (OMA V 1024−1.7, Princeton Instruments). Spectra of ThOS and ThOSe at visible wavelengths and of ThOTe at IR wavelengths can be found in Figure 1. Spectra of ThOTe at visible wavelengths and of ThOS at IR wavelengths were acquired as controls and are available in the Supporting Information.

Theoretical Calculations. Bond valences were calculated from standard parameters[21] as a simple empirical measure of oxidation state. The bond valence of an atom, V, is defined as the sum of the individual bond valences, v_i, surrounding the atom: $V = \sum v_i$. Individual bond valences were calculated from experimental bond lengths, R_i, and empirical parameters, R_0, which are unique to each atom pair: $v_i = \exp[(R_0 - R_i)/0.37]$. The parameter R_0 for the atom pairs Th−O, Th−S, Th−Se, and Th−Te was 2.167, 2.64, 2,76, and 2.94 Å, respectively.[21]

Periodic spin-polarized band structure calculations were performed with the use of the first principles DFT program VASP (Vienna *ab initio* simulation package); pseudopotentials were applied with a plane-wave basis.[22−25] The exchange correlation potential was chosen as the generalized gradient approximation (GGA) in a projector augmented wave (PAW) method, specifically GGA (PW91).[26,27] Relativistic core pseudopotentials were used. In selected cases a perturbative treatment of spin−orbit coupling was made, after lattice relaxations had converged. Automatically generated Monkhorst−Pack grids were used to carry out Brillouin zone integrations.[28] 6 × 6 × 6 k-point meshes were chosen for relaxations, total energy calculations, establishing convergence, energy comparisons, and DOS analysis. Ionic relaxation convergence was established when Hellmann−Feynman forces on each ion relaxed below 0.02 eV/Å. Additionally for ThOS, an onsite Coulomb correction to the Th 5f shell, that is the Hubbard U term,[29] was implemented in the rotationally invariant approach where the onsite Coulomb term U and onsite exchange term J were treated together as $U_{eff} = U − J$.[30] Because the 5f shell is nominally unoccupied, we expected that the effects of U_{eff} on optical properties, such as the band gap, would be minimal. It was nevertheless important to check this by direct calculation.

In the calculations, the electrons described as core in the PAW potentials were those composed of $[Xe]5d^{10}4f^{14}$ for Th, leaving 12 valence elections per atom as $6s^2p^6d^27s^2$; [He] for O, leaving six valence electrons as $2s^2p^4$; [Ne] for S, leaving six valence electrons as $3s^2p^4$; $[Ar]3d^{10}$ for Se, leaving six valence electrons as $4s^2p^4$; and $[Kr]4d^{10}$ for Te, leaving six valence electrons as $5s^2p^4$. Calculations were conducted on the 6-atom periodic crystallographic unit cell in the tetragonal space group P4/nmm; atomic positions within the fixed 100 K unit cell were relaxed to their lowest energy positions.

Oxidation states as ionic charges were determined by volume integration of electron density with the use of both atomic sphere integrations with radii, R_{WS}, and Bader's topological atom method.[31−33] Rather than dividing space into hard spheres (R_{WS}), the approach of Bader is to divide space into atomic regions determined by zero-flux charge-density surfaces.[31] Using these two methods, we define the oxidation state as the difference between the number of valence electrons contained within a volume and the number assigned to the neutral atom. The values of R_{WS} were initially set to the standard radii[34] and then increased to fill the unit-cell volume. Final values of R_{WS} were chosen as 1.5, 1.6, 1.8, 1.8, and 1.8 Å for Th, O, S, Se, and Te, respectively. The radii of S, Se, and Te were set to the same value to enable a consistent comparison among the chalcogenides.

■ RESULTS AND DISCUSSION

Syntheses. Because of the oxophylicity of Th and the stability of the ThOQ compounds, these are often the major products in reactions involving Th and a chalcogen with or without a variety of other elements when such reactions are carried out in fused-silica tubes, even if such tubes are carbon-coated. This is apparent in the present syntheses.

The reaction that yielded ThOS contained, in addition to Th and S, Ge and NaBr. The Ge was present because the reaction was intended as an exploration of the Th/Ge/S system with NaBr as flux. The reaction that yielded ThOSe contained, in addition to Th and Se, Fe and CsCl. The Fe was present because the reaction was intended to synthesize ThFeSe$_3$. The reaction that yielded ThOTe contained only Th and Te and was intended to synthesize ThTe$_2$. The most likely oxygen source in the reactions was the fused-silica tubes, because the reaction tubes were etched despite being carbon-coated.

Experimental Structures. The ThOQ compounds crystallize with two formula units in the tetragonal space group P4/nmm. They adopt the PbFCl structure with Th, O, and Q in place of Pb, F, and Cl, respectively. The site symmetries of Th, O, and Q are 4mm, 4mm, and $\bar{4}m2$, respectively. The unit-cell
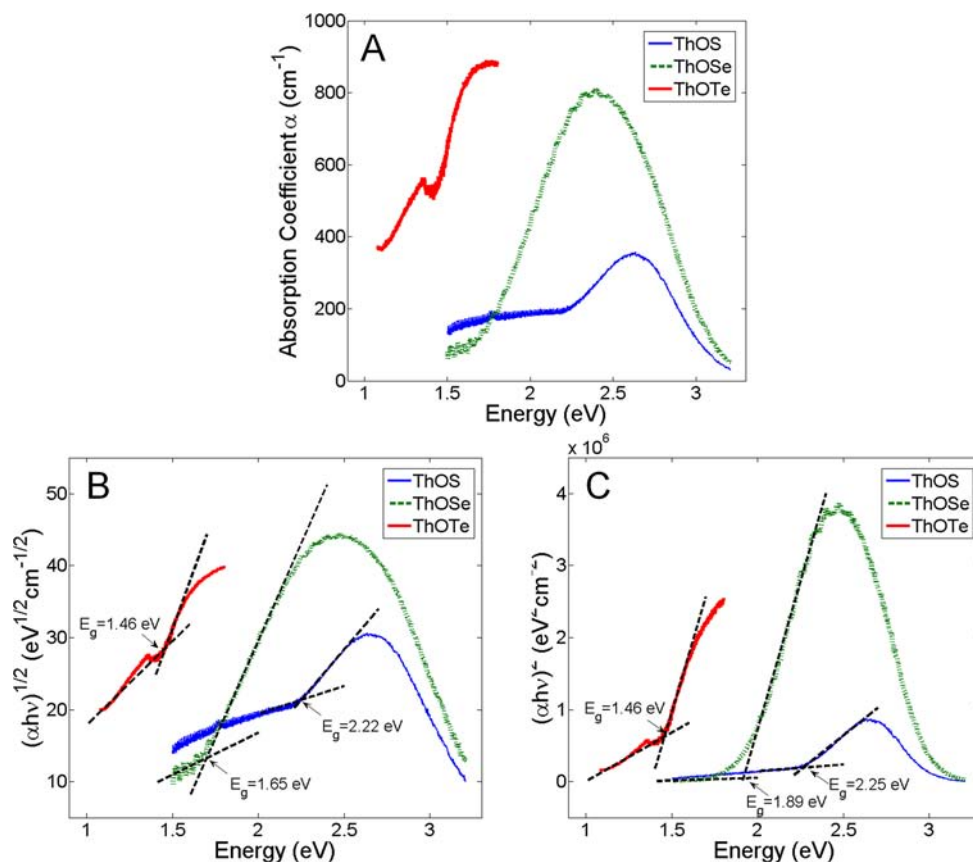
Figure 1. (A) Absorbance vs energy (eV), (B) the spectra calculated for a direct band gap, and (C) spectra calculated for an indirect direct band gap for ThOS, ThOSe, and ThOTe. The spectra calculated for an indirect band gap more closely resemble the observed absorbance spectra.

dimensions are listed in Table 1. These are plotted along with those for AnOQ (An = U, Np; Q = S, Se)[1] in Figure 2. The
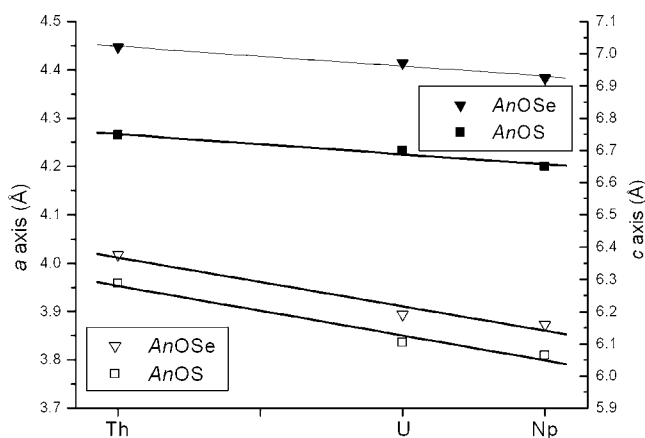

Figure 2. Comparison of axial lengths for AnOQ (An = Th, U, Np; Q = S, Se).

contraction of the actinide radius with Z is evident from these lattice constants. As seen in Figure 3, each Th atom is connected to four O and five Q atoms in a distorted monocapped square antiprism. Adjacent ThO_4Q_5 units share one O and two Q atoms with each other in the ab plane to form a layer. Each capping Q atom also forms one of the corners of the base of an ThO_4Q_4 antiprism in the layer above to create a double layer of ThO_4Q_5 units that share two Q atoms between the layers.
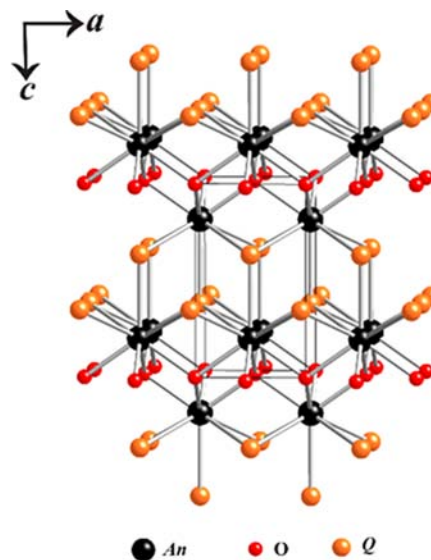

Figure 3. Structure of ThOQ viewed down the b-axis. The unit cell is outlined.

Interatomic distances for ThOQ are listed in Table 2. Each Th atom is equidistant from four Q atoms with a fifth Q atom as a cap. In ThOSe and ThOTe the capping distance is longer and in ThOS it is shorter than the distance to the other four Q atoms.

The Th−O and Th−Q distances are similar to those in ThO_2 and the Th_xQ_y binaries. The Th−O distance in ThOQ varies between 2.3981(2) and 2.4287(3) Å whereas in ThO_2 it

**Table 2. Interatomic Distances in ThOQ (Q = S, Se, Te)**

distance (Å)	ThOS	ThOSe	ThOTe
Th − O × 4	2.3981(2)	2.4095(4)	2.4287(3)
Th − Q × 4	3.002(1)	3.0916(8)	3.2593(5)
Th − Q (cap)	2.952(3)	3.139(2)	3.486(1)

is 2.4237(1) Å.[35] The Th−Q (noncapping Q) distances in ThOS, ThOSe, and ThOTe are 3.002(1), 3.0916(8), and 3.2593(5) Å, respectively. In ThS_2, $ThSe_2$, and Th_7Te_{12} the Th−Q distance varies from 2.796(1) to 3.2353(9), 2.8598(1) to 3.2882(1), and 3.187(2) to 3.459(2) Å, respectively.[5,6,36] The present metrical data for ThOQ (Q = S, Se, Te) agree with data previously obtained for the compounds, mainly from X-ray powder diffraction studies. Only for ThOTe was there an earlier single-crystal X-ray diffraction study, and the comparison to this work is made in Table 3.

Table 3. Comparison of Two Single-Crystal X-ray Structure Determinations of ThOTe

reference	this work	ref. [10]
a (Å)	4.1173(3)	4.128(2)
c (Å)	7.5289(6)	7.558(7)
Th−O (Å)	2.4287(3)	2.435(1)
Th−Te (Å)	3.2593(5)	3.268(1)
Th−Te (cap) (Å)	3.486(1)	3.507(3)
T (K)	100(2)	293 ?
$R(F)$	0.0130	0.042

Optical Measurements. ThOS, ThOSe, and ThOTe are yellow-, orange-, and black-colored, respectively. Representative photographs of crystals are shown in Figure 4.
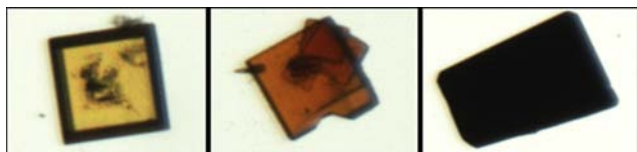
Figure 4. From left to right: Crystals of ThOS, ThOSe, and ThOTe.

A fundamental absorption edge is clearly visible for transmission through the (001) crystal face of single crystals of ThOS, ThOSe, and ThOTe (Figure 1A). Extrapolation to the absorption edge shows that ThOQ (Q = S, Se, Te) are semiconductors. Comparison of plots of absorbance vs energy to plots of $(\alpha h\nu)^{1/2}$ and $(\alpha h\nu)^2$ vs energy $(h\nu)$ provides insight on the nature of the optical transition. Because of the superior resemblance of the original absorbance data to an indirect transition plot $((\alpha h\nu)^{1/2}$ vs $h\nu)$, indirect optical band gaps of 2.22, 1.65, and 1.46 eV are assigned for ThOS, ThOSe, and ThOTe, respectively. Fits to the direct transition data yield slightly different values for ThOS and ThOSe of 2.25 and 1.89 eV, respectively. The bandgaps shown in Figures 1B and 1C were averaged over three measurements for a single crystal of ThOS and over two measurements for single crystals of ThOSe and ThOTe (see Supporting Information). No polarization dependence was observed when the polarization of visible light was scanned from 0 to 180°, and the experimental values are consistent with the colors of the compounds.

Theoretical Calculations. Calculated bond valence sums for the atoms in ThOQ (Q = S, Se, Te) are shown in Table 4.

The average bond valences for the atoms Th, O, and Q, are +4.01, −2.06, and −1.95, respectively, which support the formulation of ThOQ as $Th^{4+}O^{2-}Q^{2-}$.

Table 4. Oxidation State Calculations in ThOQ: Bader, Wigner-Seitz (W−S), and Bond Valence

compound	element	Bader	W−S	bond valence
ThOS	Th	+2.49	+3.56	+4.07
	O	−1.30	−2.24	−2.14
	S	−1.18	−0.94	−1.93
ThOSe	Th	+2.39	+3.56	+4.07
	O	−1.33	−2.18	−2.08
	Se	−1.06	−0.50	−1.99
ThOTe	Th	+2.25	+3.56	+3.89
	O	−1.33	−2.08	−1.97
	Te	−0.93	+0.30	−1.92

A more quantitative analysis follows from integration of the self-consistent electronic charge density. The calculated ionic charge of each atom from both R_{WS} volume integration and the Bader topological method may be found in Table 4. The R_{WS} integration summed to 23.62, 23.12, and 22.22 electrons out of a total of 24 valence electrons/cell for the compounds ThOS, ThOSe, and ThOTe, respectively. The "missing" 0.38 to 1.78 electrons are to be found in the interstitial region. The increase in the calculated interstitial charge S < Se < Te results from the selection of equal chalcogen radii. This choice of R_{WS} allows constant-volume comparisons, which verify the sequential expansion of electron density about the chalcogen site. This is evident in Table 4 as the R_{WS} charge on the chalcogen becomes more positive on going from S to Te, whereas the charge on Th is unchanged and that on O barely changes (0.16 e^-). At the same time, the Th−O distance stays nearly constant in the three structures, whereas the Th−Q distance increases on going from S to Se and even more from Se to Te. This demonstrates that the Th−Q bond becomes more covalent, S < Se < Te, with increased interstitial and shared electron density between Th and Q.

The Bader method divides space into atomic regions determined by zero-flux charge-density surfaces.[31] The volume of integration is not constant for the same atom in all three compounds as it was in the R_{WS} method. However, the entire cell volume is taken into account, and all electrons are accounted for. Calculation of formal oxidation states using the Bader charges gives unreasonable (i.e., nontraditional) oxidation states: averaging the values for Th, O, and Q gives $Th^{2.4+}O^{1.3-}Q^{1.1-}$. Despite the problematic charges, conclusions can be drawn about the electron distribution. As seen from the data in Table 4, as the size of Q increases, S < Se < Te, Th gains electrons, O does not change, and Q loses electrons. For O to retain the same charge, either the electron volume must change (with a corresponding change in electron density) or the volume (and electron density) appropriated to O must stay the same. The latter is more likely as the Th−O distance and the environment about O are constant in each structure. Because the Th−Q bond distance increases S < Se < Te, the volume appropriated to both Th and Q increases. As O and Q are only bonded to Th and not to each other (the shortest Q−Q distance being 3.3639(1) Å) it is evident that electron density moves from Q to Th. This means that more electrons are localized on the Th—either closer to Th than Q in the Th−Q

bond or in nonbonding orbitals—and the Th−Q bond becomes more covalent, S < Se < Te.

Densities of States. Plots of the partial densities of states (PDOS) for each atom type in ThOQ are found in Figures 5, 6,
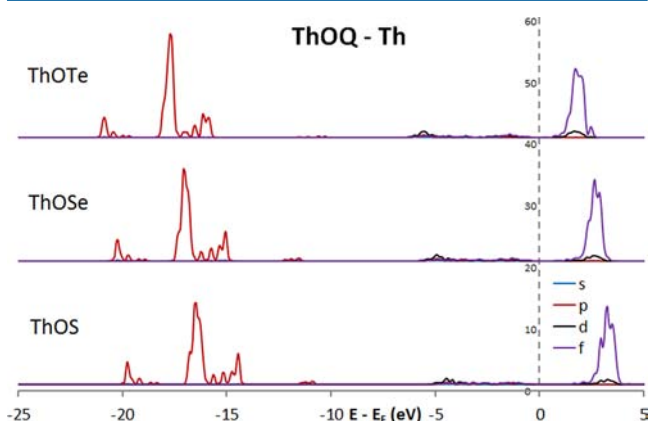

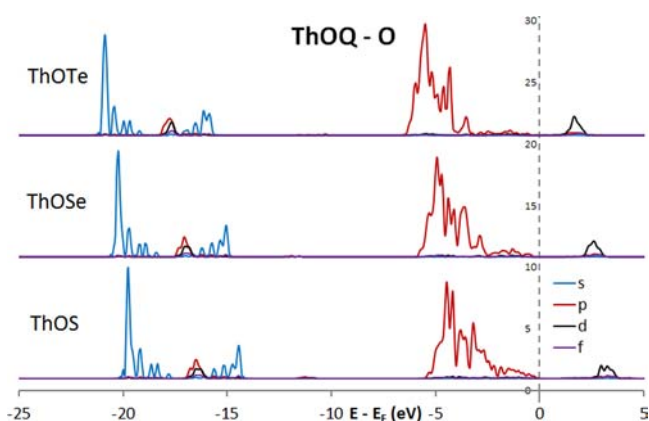**Figure 5.** Density of States for Th in ThOQ.

Figure 6. Density of States for O in ThOQ.

and 7. Each figure compares the PDOS of a different element for all three compounds. The PDOS are further separated into contributions for orbitals of s, p, d, and f character. The PDOS for both Th and O vary little among the three compounds, with the shapes and intensities of the bands being the same. They do vary in energy relative to the Fermi energy, E_F, (set to 0 eV) in the sequence Te < Se < S; a net shift of ~2 eV clearly is
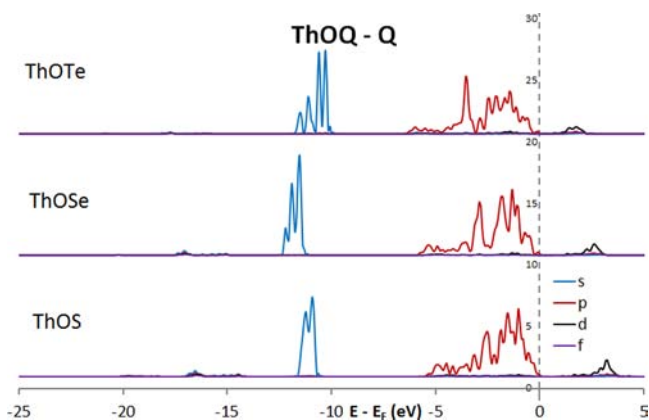

Figure 7. Density of States for Q in ThOQ.

correlated with Th−Q covalency. The upper valence band (UVB, mostly p-character) for Q varies somewhat in shape but not in overall width. The lower valence bands (LVB, mostly s-character) are rather narrow owing to lack of overlap/interaction with Th or O states.

The UVB states from −6 to 0 eV are almost exclusively due to p-orbitals of O and Q; these heavily overlap, suggesting strong hybridization between these orbitals. Starting at approximately −11 eV one finds the rather narrow LVB with a large Q s-orbital contribution and nearly zero overlap from Th and O. The ~2 eV LVB bandwidth is attributed mostly to Q−Q interactions. The deep-lying states from −21 to −14 eV are almost exclusively from the p-orbitals mixing with s-, p-, and (a small amount of) d-orbitals of O. The p- and d-orbitals of O overlap with the p-orbital of Th but not with their own s-orbital; that is, there seems to be little O s-p hybridization. The O 2s-orbital dominates the contribution of overlap with the Th p-orbital.

The unoccupied states from 0 to 4 eV above E_F are dominated by empty Th f-orbitals with a small but non-negligible contribution from empty d-orbitals of Th, O, and Q.

Theoretical Band Gaps. In all three compounds the smallest band gap is direct and occurs at the k-space zone center Γ with values of 1.09, 0.75, and 0.17 eV for ThOS, ThOSe, and ThOTe, respectively. The three next highest band gaps for all three compounds are two indirect transitions from Γ to $(0\ 0\ 1/6) = \zeta$ and a $\zeta - \zeta$ direct gap. The values for these band gaps are 1.18, 1.19, and 1.28 eV for ThOS; 0.83, 0.85, and 0.93 eV for ThOSe; and 0.23, 0.27, and 0.33 eV for ThOTe. The low-lying excitations are essentially from chalcogen Q p-states to Th f-states, in accord with simple ionic models with the $Th^{4+}6p^66d^07s^05f^0$ configuration. In agreement with experiment, one sees a trend to lower energy down the chalcogen series. The calculated values are systematically smaller than experiment, as frequently observed in DFT modeling. The origins of the band gap errors in DFT are well-known, and related to the difference in effective potentials seen by occupied and vacant states. The so-called DFT+U methodology introduces an explicit correlation term, generally parametrized, to expand the gap.

For ThOS, electronic states were recalculated after the introduction of the (somewhat large) Hubbard U parameter of value 4 eV for Th f-states. In actinide compounds, the Hubbard U parameter is typically used to introduce a gap between occupied and vacant f-states. As expected for Th, introducing the U term for Th f-states had essentially no effect on the spectra as described by the PDOS (Figures 8A and 8B), as Th has virtually no occupied f orbitals. The difference in the calculated band gap turned out to be negligible; the value for the lowest band gap was 1.13 eV with the Hubbard U term and 1.09 eV without. The same lack of a major effect is expected for the introduction of the U term in ThOSe and ThOTe. This is clearly a case where a single-site correlation correction for the excited state energies is inadequate; multiple-site corrections are beyond the scope of this work.

As described above, low-lying transitions have been calculated at approximately 1.1 eV for ThOS. However, examination of the PDOS shows that the spectral weight of these transitions is very small, and that the main absorption onset occurs from a Q p-band to a Th f-band at approximately 2 eV, close to values extrapolated from experimental data. Similarly, the main absorption as evident from the PDOS of ThOSe and ThOTe occurs at approximately 1.5 and 0.75 eV,
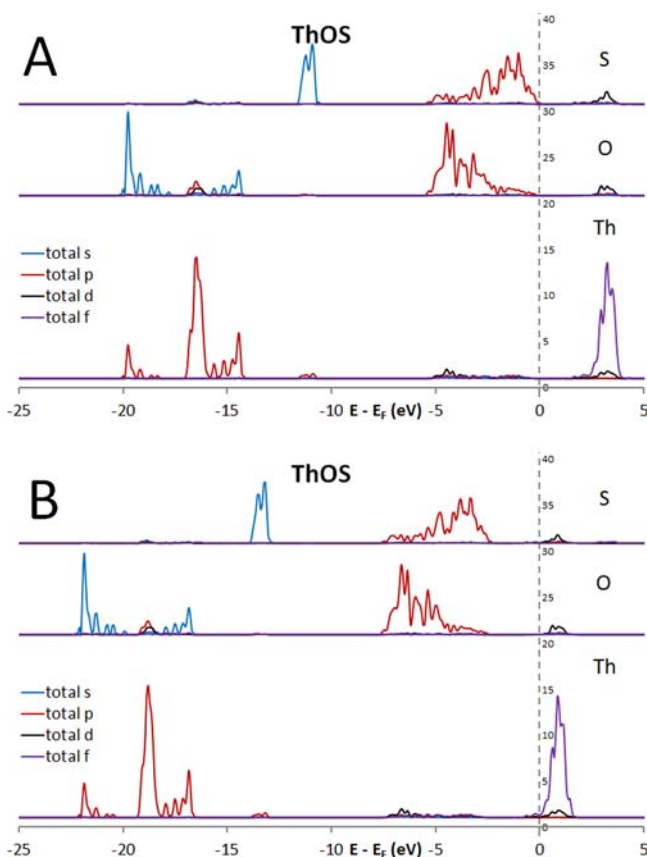
Figure 8. Comparison of Density of States for ThOQ (A) without and (B) with the Hubbard U parameter of 4 eV.

respectively. A summary of calculated and experimental band gaps is found in Table 5.

Table 5. Summary of Theoretical and Experimental Band Gaps (eV) Found in ThOQ (Q = S, Se, Te)

type			ThOS	ThOSe	ThOTe
calculated (four lowest)	direct		1.09^a	0.75	0.17
	indirect		1.18	0.83	0.23
	indirect		1.19	0.85	0.27
	direct		1.28	0.93	0.33
strong onset from PDOS			~2	~1.5	~0.75
from optical^b	indirect		2.22	1.65	1.46
	direct		2.25	1.89	1.46

^{a}Lowest band gap from the calculation containing the Hubbard U term was 1.13 eV. ^{b}The indirect transition fits absorbance data better.

CONCLUSIONS

The compounds ThOS, ThOSe, and ThOTe were synthesized as side products in multiple reactions. Their structures have been determined by means of single-crystal X-ray diffraction methods. All three compounds adopt the PbFCl structure type in the tetragonal space group $D_{4h}^7 - P4/nmm$. More precise crystallographic data have been obtained for ThOS and ThOSe, which had previously only been known from X-ray powder diffraction data. ThOS, ThOSe, and ThOTe are yellow-, orange-, and black-colored, respectively. From single-crystal optical absorption measurements the indirect band gaps are 2.22, 1.65, and 1.45 eV, respectively; these are consistent with

their colors. Extrapolation to the absorption edge shows that each compound is a semiconductor. Calculated bond valence sums for the atoms in ThOQ (Q = S, Se, Te) lead to average bond valences for the atoms Th, O, and Q of +4.01, −2.06, and −1.95, respectively, which support the formulation of ThOQ as $Th^{4+}O^{2-}Q^{2-}$. Periodic spin-polarized band structure calculations were performed with the use of the first principles DFT program VASP. The calculated ionic charge of each atom from both R_{WS} volume integration and the Bader topological method demonstrates that the Th−Q bond becomes more covalent, S < Se < Te, with increased interstitial and shared electron density between Th and Q. The calculated band gaps are systematically smaller than experiment, as is frequently observed in DFT modeling.

■ ASSOCIATED CONTENT

Ⓢ Supporting Information

Details on the bandgaps shown in Figures 1B and 1C. Spectra of ThOTe at visible wavelengths and of ThOS at IR wavelengths. The crystallographic files in CIF format for ThOS, ThOSe, and ThOTe. This material is available free of charge via the Internet at http://pubs.acs.org.

■ AUTHOR INFORMATION

Corresponding Author

*E-mail: ibers@chem.northwestern.edu.

Notes

The authors declare no competing financial interest.

■ REFERENCES

(1) Jin, G. B.; Raw, A. D.; Skanthakumar, S.; Haire, R. G.; Soderholm, L.; Ibers, J. A. *J. Solid State Chem.* **2010**, *183*, 547−550.
(2) Trzebiatowski, W.; Niemiec, J.; Sepichowska, A. *Bull. Acad. Pol. Sci., Ser. Sci. Chim.* **1961**, *9*, 373−377.
(3) Marcon, J.-P. *C. R. Seances Acad. Sci., Ser. C* **1967**, *265*, 235−237.
(4) Gorum, A. E. *Acta Crystallogr.* **1957**, *10*, 144.
(5) Amoretti, G.; Calestani, G.; Giori, D. C. *Z. Naturforsch. A: Phys. Phys. Chem. Kosmophys.* **1984**, *39*, 778−782.
(6) D'Eye, R. W. M. *J. Chem. Soc.* **1953**, *75*, 1670−1672.
(7) Graham, J.; McTaggart, F. K. *Aust. J. Chem.* **1960**, *13*, 67−73.
(8) Zachariasen, W. H. *Acta Crystallogr.* **1949**, *2*, 291−296.
(9) D'Eye, R. W. M.; Sellman, P. G.; Murray, J. R. *J. Chem. Soc.* **1952**, *74*, 2555−2562.
(10) Beck, H. P.; Dausch, W. *Z. Anorg. Allg. Chem.* **1989**, *571*, 162−164.
(11) Eastman, E. D.; Brewer, L.; Bromley, L. A.; Gilles, P. W.; Lofgren, N. L. *J. Am. Chem. Soc.* **1951**, *73*, 3896−3898.
(12) Boelsterli, H. U.; Hulliger, F. *J. Mater. Sci.* **1968**, *3*, 664−665.
(13) Gensini, M.; Gering, E.; Benedict, U.; Gerward, L.; Staun, O. J.; Hulliger, F. *J. Less-Common Met.* **1991**, *171*, L9−L12.

8117

dx.doi.org/10.1021/ic300510x | *Inorg. Chem.* 2012, 51, 8112−8118

(14) Amoretti, G.; Giori, D. C.; Varacca, V.; Spirlet, J. C.; Rebizant, J. *Phys. Rev. B* **1979**, *20*, 3573−3578.

(15) Amoretti, G.; Blaise, A.; Collard, J. M.; Hall, R. O. A.; Mortimer, M. J.; Troc, R. *J. Magn. Magn. Mater.* **1984**, *46*, 57−67.

(16) Witt, R. H.; Nylin, J.; McCullough, H. M. *A Study of the Hydride Process for Producing Thorium Powder*; United States Atomic Energy Commission, Atomic Energy Division, Sylvania Electric Products, Inc.: Bayside, NY, 1956.

(17) *Bruker APEX2 Version 2009.5-1 and SAINT version 7.34a Data Collection and Processing Software*; Bruker Analytical X-Ray Instruments, Inc.: Madison, WI, 2009.

(18) *Bruker SMART Version 5.054 Data Collection and SAINT-Plus Version 6.45a Data Processing Software for the SMART System*; Bruker Analytical X-Ray Instruments, Inc.: Madison, WI, 2003.

(19) Sheldrick, G. M. *Acta Crystallogr., Sect. A: Found. Crystallogr.* **2008**, *64*, 112−122.

(20) Gelato, L. M.; Parthé, E. *J. Appl. Crystallogr.* **1987**, *20*, 139−143.

(21) Brese, N. E.; O'Keeffe, M. *Acta Crystallogr., Sect. B: Struct. Sci.* **1991**, *47*, 192−197.

(22) Kresse, G.; Hafner, J. *Phys. Rev. B* **1993**, *47*, 558−561.

(23) Kresse, G.; Hafner, J. *Phys. Rev. B* **1994**, *49*, 14251−14271.

(24) Kresse, G.; Forthmüller, J. *Comput. Mater. Sci.* **1996**, *6*, 15−50.

(25) Kresse, G.; Furthmüller, J. *Phys. Rev. B* **1996**, *54*, 11169−11186.

(26) Kresse, G.; Joubert, D. *Phys. Rev. B* **1999**, *59*, 1758−1775.

(27) Perdew, J. P. In *Electronic Structure of Solids*; Ziesche, P.; Eschrig, H., Eds.; Akademie Verlag: Berlin, Germany, 1991; pp 11−20.

(28) Monkhorst, H. J.; Pack, J. D. *Phys. Rev. B* **1976**, *13*, 5188−5192.

(29) Hubbard, J. *Proc. R. Soc. London, Ser. A* **1963**, *276*, 238−257.

(30) Dudarev, S. L.; Botton, G. A.; Savrasov, S. Y.; Humphreys, C. J.; Sutton, A. P. *Phys. Rev. B* **1998**, *57*, 1505−1509.

(31) Henkelman, G.; Arnaldsson, A.; Jónsson, H. *Comput. Mater. Sci.* **2006**, *36*, 354−360.

(32) Sanville, E.; Kenny, S. D.; Smith, R.; Henkelman, G. *J. Comput. Chem.* **2007**, *28*, 899−908.

(33) Bader, R. F. W. *Atoms in molecules: a quantum theory*; Oxford University Press, Inc.: New York, 1990.

(34) Shannon, R. D. *Acta Crystallogr., Sect. A: Cryst. Phys. Diffr. Theor. Gen. Crystallogr.* **1976**, *32*, 751−767.

(35) Taylor, D. *Br. Ceram. Trans. J.* **1984**, *83*, 32−37.

(36) Tougait, O.; Potel, M.; Noël, H. *Inorg. Chem.* **1998**, *37*, 5088−5091.

8118

dx.doi.org/10.1021/ic300510x | *Inorg. Chem.* 2012, 51, 8112−8118